

Highly Robust, Automated, and Sensitive Online TiO₂-Based Phosphoproteomics Applied To Study Endogenous Phosphorylation in *Drosophila melanogaster*

Martijn W. H. Pinkse,[†] Shabaz Mohammed, Joost W. Gouw, Bas van Breukelen, Harmjan R. Vos, and Albert J. R. Heck*

Department of Biomolecular Mass Spectrometry, Bijvoet Center for Biomolecular Research and Utrecht Institute for Pharmaceutical Sciences, Utrecht University, Sorbonnelaan 16, 3584 CA Utrecht, The Netherlands

Received September 17, 2007

Reversible protein phosphorylation ranks among the most important post-translational modifications, and elucidation of phosphorylation sites is essential to understand the regulation of key cellular processes such as signal transduction. Enrichment of phosphorylated peptides is a prerequisite for successful analysis due to their low stoichiometry, heterogeneity, and low abundance. Enrichment is often performed manually, which is inherently labor-intensive and a major hindrance in large-scale analyses. Automation of the enrichment method would vastly improve reproducibility and thereby facilitate 'high-throughput' phosphoproteomics research. Here, we describe a robust and automated online TiO₂-based two-dimensional chromatographic approach to selectively enrich phosphorylated peptides from digests of complete cellular lysates. We demonstrate method enhancement for both adsorption and desorption of phosphorylated peptides resulting in lower limits of detection. Phosphorylated peptides from a mere 500 attomole tryptic digest of a protein mixture were easily detected. With the combination of strong cation exchange chromatography with the online TiO₂ enrichment, 2152 phosphopeptides were enriched from 250 μg of protein originating from the cell lysate of *Drosophila melanogaster* S2 cells. This is a 4-fold improvement when compared to an enrichment strategy based solely on strong cation exchange/LC-MS. Phosphopeptide enrichment methods are intrinsically biased against relatively basic phosphopeptides. Analysis of the *pI* distributions of the enriched/detected phosphopeptides showed that the *pI* profile resembles that of a total *Drosophila* protein digest, revealing that the current described online procedure does not discriminate against either more acidic or basic phosphopeptides. However, careful comparison of our new and existing phosphopeptide enrichment techniques also reveal that, like many enrichment techniques, we are still far from comprehensive phosphoproteomics analyses, and we describe several factors that still require to be addressed. Still, as the online approach allows the complementary measurements of phosphopeptides and their nonphosphorylated counterparts in subsequent analyses, this method is well-suited for automated quantitative phosphoproteomics.

Keywords: TiO₂ phosphopeptide enrichment • Automated, Large Scale • Phosphoproteomics • Phosphopeptide iso-electric point

Introduction

Identification and site location within phosphopeptides is important for investigating the influence of reversible protein phosphorylation and the global understanding of the regulatory process mediated by protein kinases and phosphatases. Continuous developments in effective and robust enrichment techniques in conjunction with significant improvements of mass spectrometers have allowed phosphoproteomics research to become a more common practice in many research labo-

ratories. Specific enrichment of phosphorylated peptides remains a challenging and highly relevant task in phosphoproteomic-related questions. Various techniques and strategies are available that have been specifically developed to isolate and enrich phosphorylated peptides and proteins, all with their own advantages and disadvantages (for reviews see refs 1–6). To make phosphoproteomics amenable to nonspecialists the development of routine automated enrichment protocols is highly desirable. Immobilized metal ion affinity chromatography (IMAC) is the most frequently used method for phosphopeptide enrichment.^{7,8} However, IMAC protocols vary widely in metal-charging, washing, and eluting conditions and may require significant experience to work effectively. In addition, nonspecific binding of acidic/nonphosphorylated peptides

* To whom correspondence should be addressed. Tel., 31-30-2536797; fax, 31-30-2518219; e-mail, a.j.r.heck@uu.nl.

[†] Present address: Analytical Biotechnology, Delft University of Technology, Julianalaan 67, 2628 BC Delft, The Netherlands.

often hampers successful analysis. Recently, TiO₂ was introduced as an effective material to isolate phosphorylated peptides from proteolytic digests.^{9,10} In a direct comparison with IMAC, it was shown that TiO₂ has a far higher capacity and better selectivity toward phosphorylated peptides.¹¹ Just like IMAC-methods, many of the reported TiO₂ strategies are based on the off-line manual performance of the enrichment using self-packed^{11–13} or commercially available^{14,15} TiO₂-microcolumns. The success and reproducibility of these approaches depends on serious efforts and time from the researcher and often require adjustments to the specific samples analyzed. In addition, for large-scale analysis in which large amounts of samples need to be analyzed, many sample handling steps have to be done manually, which is evidently labor-intensive and could lead to irreproducible results. Within this context, automation of the enrichment protocol would allow reproducibility, unattended operation, and subsequently higher throughput. Online IMAC–reversed phase–mass spectrometric setups have been introduced, but often involve complicated analytical setups with multiple pumps, solvents, and switching valves.^{16,17} Here, we report an automated nanoflow 2D-LC-system for the selective enrichment of phosphorylated peptides. This fully automated setup is easily adapted onto existing nanoflow setups and does not require complicated plumbing and/or column switching. The enrichment efficiency is highly reproducible, allowing many analyses using one and the same TiO₂-precolumn. Furthermore, the automated procedure allows a full characterization for each sample, since both flow-through (i.e., nonphosphorylated peptides) and TiO₂-eluate (phosphorylated peptides) are analyzed. This is especially important in quantitative phosphoproteomics, since there is a need to discriminate between changes in protein phosphorylation and changes in protein abundance. In addition, our method provides a continuous quality control of the enrichment efficiency. A simple regeneration step allows robust and reproducible analyses with attomole sensitivity. The method is directly applicable for the analysis of complex mixtures such as total cellular extracts, as demonstrated for a cellular extract of *Drosophila melanogaster* S2 cells. Prior to the online-TiO₂ analysis, a highly complex peptide sample was first subfractionated via strong cation exchange (SCX). SCX itself enriches to a large extent for phosphopeptides, because below pH 3.0, their overall solution-charge state is lower than the average nonphosphorylated tryptic peptide. In combination with LC–MS, SCX was shown to greatly enhance detection of phosphorylated peptides.¹⁸ In combination with either IMAC or TiO₂, followed by LC–MS, even higher levels of enrichment can be achieved.^{19–21} In the present study, we subjected our automated online-TiO₂ phosphopeptide enrichment strategy to the analysis of cytosolic proteins from *D. melanogaster* S2 cells. A total of 2152 phosphorylated peptides were retained and subsequently detected via the online approach. Analysis of the *pI* distributions of the enriched/detected phosphopeptides showed that the obtained *pI* profile closely resembles that of a total *Drosophila* protein digest, revealing that our online procedure is relatively unbiased toward either more acidic or basic phosphopeptides.

Experimental Procedures

Material and Reagents. Sequencing grade trypsin was purchased from Roche Diagnostics (Ingelheim, Germany). Bovine serum albumin, bovine alpha and beta casein, porcine glyceraldehyde dehydrogenase, and conalbumin from chicken

egg white were purchased from Sigma-Aldrich (Zwijndrecht, The Netherlands). RKIpSASEF was from Neosystem Laboratoire (Strasbourg, France). 2,5-Dihydroxy benzoic acid, ammonium bicarbonate, sodium phosphate, potassium fluoride, potassium chloride, sodium orthovanadate, acetic acid, and formic acid were from Sigma (Zwijndrecht, The Netherlands). Titanium oxide (Titansphere, 10 μm) was a gift from GL-science (GL-Sciences, Inc., Japan). Aqua C18, 5 μm, 200 Å, (Phenomenex, Torrance, CA) resin was used for the trap column, and ReproSil-Pur C18-AQ, 3 μm, 120 Å, (Dr. Maisch GmbH, Ammerbuch, Germany) resin was used for the analytical column. HPLC grade acetonitrile was purchased from Biosolve (Valkenswaard, The Netherlands), Potassium silicate (KASIL 1624) was purchased from PQ Europa (Winschoten, The Netherlands). Fused silica capillaries (50 and 100 μm i.d., 375 o.d.) were obtained from Bester (Amstelveen, The Netherlands).

Sample Preparations. Serum albumin, alpha and beta casein, glyceraldehyde dehydrogenase, and conalbumin (100 μM) were reduced in 1 mM DTT and alkylated in 2 mM iodoacetamide, following digestion with trypsin overnight at a protein/protease ratio of 50:1. On the day of analysis, the test mixture was prepared by dilution of the protein digests (100 μM) and the peptide RKIpSASEF (50 μM stock) to 5 fmol/μL in 0.5% formic acid. Prior to the analysis of 500 amol, the 5 fmol/μL solution was diluted 100-fold in 0.5% formic acid. *D. melanogaster* S2 cells were grown at 25 °C in Schneider's *Drosophila* medium (Gibco) supplemented with 10% heat-inactivated fetal bovine serum and penicillin (100 μg/mL)/streptomycin (100 μg/mL). Cells were harvested by centrifugation at 1500 rpm, and after removal of the medium, cells were resuspended in 1 mL ice-cold 25 mM sodium phosphate, pH 7.4. After centrifugation at 1500 rpm and removal of the supernatant, cells were lysed in 100 μL of 8 M urea and 50 mM ammonium bicarbonate, containing 5 mM sodium phosphate, 1 mM potassium fluoride, and 1 mM sodium orthovanadate, pH 8.2. Cellular debris was pelleted by centrifugation at 14 000 rpm for 20 min. Approximately 1 mg of protein material was digested and was, after separation by SCX, split into four aliquots which were used for the individual analyses. Prior to digestion, proteins were reduced with 1 mM DTT and alkylated with 2 mM iodoacetamide. The mixture was diluted 4-fold to 2 M urea using 250 μL of 50 mM ammonium bicarbonate and 50 μL of trypsin solution, 0.1 mg/mL, and incubated overnight at 37 °C.

Strong Cation Exchange. Strong cation exchange was performed using a Zorbax BioSCX-Series II column (0.8 mm i.d. × 50 mm length, 3.5 μm), a FAMOS autosampler (LC-packing, Amsterdam, The Netherlands), a Shimadzu LC-9A binary pump and a SPD-6A UV-detector (Shimadzu, Tokyo, Japan). Prior to SCX chromatography, protein digests were desalted using a small plug of C18 material (3 M Empore C18 extraction disk) packed into a GELoader tip (Eppendorf) similar to what has been previously described,²² onto which ~10 μL of Aqua C18 (5 μm, 200 Å) material was placed. The eluate was dried completely and subsequently reconstituted in 20% acetonitrile and 0.05% formic acid. After injection, a linear gradient of 1% min⁻¹ solvent B (500 mM KCl in 20% acetonitrile and 0.05% formic acid, pH 3.0) was performed. A total of 24 SCX fractions (1 min each, i.e., 50 μL elution volume) were manually collected and dried in a vacuum centrifuge.

2D-Nanoflow-HPLC. A home-built nanoflow vented column system, consisting of a LC-Packings Ultimate quaternary solvent

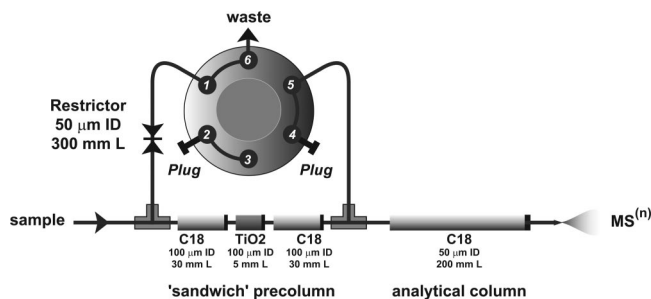


Figure 1. Schematic overview of the vented column system, using a triple stage precolumn. The ‘sandwich’ precolumn consists of three individual precolumns of C18, TiO₂, and C18 material, respectively. During analysis, all peptides are initially trapped during sample loading onto the first stage of C18. After flow-splitting, nonphosphorylated peptides are analytically separated and subsequently detected, while phosphorylated peptides are trapped on the TiO₂ precolumn at a very low flow rate. This optimal procedure allows superior binding efficiency, without increasing total analysis time.

delivery system, a thermostatted FAMOS autosampler, and a Switchos 6-Port switching module (LC-Packings, Amsterdam, The Netherlands), coupled online with a LTQ-Orbitrap mass spectrometer (Thermo Electron, Bremen, Germany), was used for all analyses. Figure 1 shows a schematic overview of the vented column switching setup. The trap column consist of three separate precolumns, a 30 mm × 100 μm Aqua C18 precolumn, followed by a 5 mm × 100 μm TiO₂ precolumn, followed by another 30 mm × 100 μm Aqua C18 precolumn. The ‘sandwich’ precolumn is then coupled with a 200 mm × 50 μm ReproSil-Pur C18-AQ analytical column. Peptides were trapped at 3 μL/min in 100% solvent A (0.1 M acetic acid and 0.46 M formic acid in water) on the first 30 mm C18 trap column. The subsequent H₂O/ACN gradient will elute and separate the bound peptides using the analytical column at a flow rate of ~100 nL min⁻¹. Note: phosphorylated peptides will enter the TiO₂ precolumn at this flow rate and bind to the resin. The low flow rate allows better conditions for binding when compared with direct loading of the sample onto a TiO₂ precolumn at a typical flow rate of 1–5 μL min⁻¹. All other peptides, with no TiO₂ affinity, are chromatographically separated at ~100 nL/min in a 70-min gradient from 0 to 40% solvent B (80% acetonitrile, 0.1 M acetic acid + 0.46 M formic acid). Elution of phosphorylated peptides is achieved by injection of 30 μL of 250 mM ammonium hydrogen bicarbonate, pH 9.0 (adjusted with ammonia) containing 10 mM sodium phosphate, 5 mM sodium orthovanadate, and 1 mM potassium fluoride, followed by an injection of 20 μL of 5% formic acid. During a second H₂O/ACN gradient, phosphopeptides are separated using the 200 mm analytical column at ~100 nL/min in a 70-min gradient from 0 to 40% solvent B (80% acetonitrile, 0.1 M acetic acid + 0.46 M formic acid). The effluent was sprayed via distal coated emitter tips (New Objective), butt-connected to the analytical column. An additional 33 MΩ resistor was placed between the high voltage supply and the electrospray needle in order to reduce ion current.

Mass Spectrometry. The LTQ-Orbitrap mass spectrometer was operated in data-dependent mode, automatically switching between MS and MS/MS and neutral loss driven MS³ acquisition. Full scan MS spectra (from *m/z* 300–1500) were acquired in the Orbitrap with a resolution of 60 000 at *m/z* 400 after accumulation to target value of 500 000. The three most intense

ions at a threshold above 5000 were selected for collision-induced fragmentation in the linear ion trap at a normalized collision energy of 35% after accumulation to a target value of 15 000. The data-dependent neutral loss settings were chosen to trigger an MS³ event after a neutral loss of either 24.5, 32.6 of 49 ± 0.5 *m/z* units was detected among the 5 most intense fragment ions.

Peptide Identification and Validation. All MS² and MS³ spectra were converted to single DTA files using Bioworks 3.2 (Thermo, San Jose, CA). An in-house developed Perl script was used to assign the original and accurate parent mass to all MS³ spectra, enabling an accurate mass database search. Eventually, all MS² and MS³ spectra were merged into Mascot generic format files which were searched using an in-house licensed Mascot v2.2 search engine (Matrix Science) against a *D. melanogaster* database containing TrEMBL and Swiss-Prot entries (version 34.4; containing 28 946 sequences; 14 600 642 residues). Carbamidomethyl cysteine was set as a fixed modification; protein N-acetylation, N-terminal pyroglutamate, oxidized methionines, and phosphorylation of serine, threonine, or tyrosine were set as variable modifications. Trypsin was specified as the proteolytic enzyme, and up to two missed cleavages were allowed. The mass tolerance of the precursor ion was set to 10 ppm, and that of fragment ions was set to 0.9 Da. The false discovery rate was estimated using an equivalent sized database generated from random sequences;²³ this step is performed automatically by Mascot v2.2 by selecting Decoy as an additional search parameter. The false discovery rate was determined to be 1.07% at a Mascot threshold of 35. The threshold for Mascot identification was set to 35, and using an in-house developed Perl-script, the Mascot summary page was screened for phosphorylated peptides. Multiple identifications of the same peptide, including different charge states, were omitted from the count, resulting in an absolute number of unique phosphopeptides.

Phosphopeptide *pI* Analysis. Peptides containing phosphorylation sites were extracted from Mascot searches (DAT files) with an in-house built script and ranked based on their Mascot scores. Peptides with a Mascot score higher than 35 were assumed to be reliable and used for further analysis. In our experience, peptides with scores between 35 and 50 are correctly identified as phosphorylated; however, site assignment by MASCOT can be somewhat unreliable. The small proportion of inaccurately assigned phosphosites will not affect the *pI* profile. Duplicate peptides and peptides with N-terminal modifications were discarded from analyses. This resulted in 1962 unique phosphopeptides for the TiO₂ eluate, 51 for the TiO₂ flow-through, and 479 for the SCX-only. The *pI* values of the phosphopeptides were calculated using an in-house built java tool. Amino acid p*K*_a values were used as reported within refs 24 and 25; p*K*_a values for pY and pS/T are taken from ProteoMod (pY, 1.0 and 7.0, and pS/T, 2.12 and 7.12, respectively²⁶). The calculated *pI*s were binned with a *pI* range of 0.25 and plotted as a bar-graph for comparison. In addition, the *pI*s were binned in three sets named acidic, intermediate, and basic, ranging from *pI* < 5, pH 5 < *pI* < pH 7 and *pI* > 7. Three other large-scale phosphopeptide data sets used were from *D. melanogaster* Kc167 cells,²⁷ mouse liver,²⁸ and HeLa cells,²⁹ whereby for the last data set we only used the subset of reported sites that had Mascot values above 35 in order to allow a consistent comparison.

Results

Evaluation and Optimization of Phosphopeptide Binding. A frequently encountered issue in phosphopeptide enrichment techniques is the coisolation of peptides of acidic nature. This problem is both encountered in IMAC as well as TiO₂ purifications. It has been reported that in both IMAC and TiO₂ purifications, O-methyl esterification of carboxyl-groups reduces nonspecific binding significantly,^{8,9} but it is often less preferred due to incomplete yields in the chemical derivatization and potential unwanted deamidation and subsequent methylation of Asn and Gln residues.¹¹ In an off-line TiO₂-strategy, Larsen et al. demonstrated that the addition of 2,5-dihydroxybenzoic acid (DHB) in the elution solvent may substantially reduce the number of nonphosphorylated peptides detected in the phosphopeptides eluate.¹¹ This approach is not easily applicable to LC-MS, since the high concentration of DHB can cause various problems with the LC-system and/or contaminate the ion source of the mass spectrometer.^{13,15,30} Moreover, several groups have shown that, although the purity of the phosphopeptides is increased, the overall number of phosphopeptides identified is significantly reduced, when using DHB in the enrichment.^{27,30} Alternatively, 1-octanesulfonic acid¹⁵ or lactic acid³⁰ are also known to substantially decrease nonspecific binding during sample loading, albeit in off-line formats. Previously, it was shown that the addition of 2–5% formic acid to the elution solvent may also substantially decrease nonspecific binding in an off-line loading procedure.³¹ It can be safely assumed that of the above-mentioned additives, formic acid will cause the least problems in online approaches. Using an artificial sample of a synthetic phosphopeptide and a mixture of digested (phospho)proteins (see Experimental Procedures), we evaluated whether the addition of formic acid (0.5%) to the solvent system would decrease nonspecific binding and improve the capturing of phosphorylated peptides. Figure 2 shows extracted ion chromatograms obtained from 25 fmol of the mixture of the synthetic phosphopeptide and the digested (phospho)proteins, analyzed by normal LC-MS and 2D TiO₂-LC-MS. Displayed are the extracted ion-chromatograms of five phosphorylated peptides. Figure 2A displays the extracted ion chromatogram (EIC) of a normal (i.e., using only a C18 precolumn) reversed phase analysis. Panels B and C of Figure 2 display the chromatograms for the flow-through and the TiO₂-eluate, respectively, obtained using a dual precolumn (TiO₂-C18), as previously described.⁹ Analysis of the flow-through highlights that under these conditions (i.e., with 0.5% formic acid) a substantial amount of the phosphorylated peptides are not sufficiently trapped and appear in the first gradient among the majority of nonphosphorylated peptides. Although all peptides are also detected in the second run (i.e., after elution with ammonium bicarbonate), this scenario is far from ideal. Lowering the sample loading speed decreased the amount of phosphorylated peptides that broke through (data not shown); however, it did not completely prevent it. Schlosser et al. also noticed that the loading speed formed a critical parameter in the off-line approach and used a pump to allow greater control.³¹ One can imagine that when using manual TiO₂-pipet tips careful control of the loading speed is more arduous, if not impossible. In an online application, using the dual-precursor, the sample flow can be easily reduced; however, this will result in very long sample loading times. To improve the capture of phosphorylated peptides, we positioned an additional C18 precolumn in front of the TiO₂-C18 precolumn, resulting in a 'sandwich' configuration (see Figure 1). In

this case, all peptides, both phosphorylated and nonphosphorylated, will bind initially to this first stage of C18 material. During the first H₂O/ACN gradient (i.e., analysis of the flow-through), peptides will elute with a flow equal to the flow-rate within the analytical column, that is, ~100 nL/min. This flow is ~30-fold lower than the initially used sample-loading flow rate of 3 μ L/min. As a consequence, phosphorylated peptides spend much more time in the TiO₂ column, enhancing their binding efficiency. These superior binding conditions lead to far lower levels of breakthrough, and Figure 2D shows that when the same standard mixture is analyzed under 'sandwich' conditions no phosphorylated peptides are detected in the first run, while more than 90% of the bound material is recovered in the TiO₂-eluate (Figure 2E). Using the dual precolumn configuration,⁹ sample loading at a reduced flow rate of 100 nL min⁻¹ would, for a typical sample volume of 20 μ L, require a loading time of 200 min. Thus, the 'sandwich' configuration provides a major advantage in phosphopeptide binding without any compromise on sample analysis time.

Improved Elution Leads to Detection of Phosphopeptides at Attomole Sensitivity. To elute phosphorylated peptides from the TiO₂ material, typically 30 μ L of a 250 mM ammonium bicarbonate (pH 9.0) is injected over the triple precolumn.^{9,31} It is noted that this elution is not always sufficient to elute all phosphorylated peptides, including rather acidic and/or multiply phosphorylated peptides.¹¹ Supplementary Figure 1A in Supporting Information displays extracted ion chromatograms of the phosphopeptides from the peptide mixture after the elution with 30 μ L of 250 mM NH₄HCO₃, pH 9.0. While a majority of the expected phosphorylated peptides are observed, after injection of another 30 μ L of 250 mM NH₄HCO₃ again, a substantial amount of phosphorylated peptides were detected (Supplementary Figure 1B in Supporting Information), indicating the first 30 μ L elution is indeed not sufficient. Previously, it was shown that a phosphate buffer could also be used to elute the trapped phosphopeptides;¹⁰ hence, we investigated the use of phosphates and other hard Lewis bases for elution. Supplementary Figure 1C in Supporting Information shows that by using a mixture of hard Lewis bases, phosphate, vanadate, and fluoride in combination with the adjusted pH of the ammonium bicarbonate can considerably improve the yield of phosphorylated peptides. The second elution only yielded an extra 10%, highlighting the superior conditions (Supplementary Figure 1D in Supporting Information). To demonstrate the efficiency and sensitivity of the automated method for low sample amounts, 500 amol of the multiple protein tryptic digest and the synthetic peptide was analyzed using the optimized conditions (see Figure 3). Shown are the extracted ion chromatograms of the 5 phosphorylated peptides for the analysis of 25 fmol (Figure 3A) and the analysis of 500 amol (Figure 3B). At this low level, the phosphorylated peptides are still efficiently trapped and subsequently detected and sequenced in the TiO₂ elution analysis, as illustrated for the peptide YKVPQLEIVNPpSAEER in Figure 3C.

Application to a Digest of *D. melanogaster* S2 Cell. The purpose of automation is eventually to analyze large number of samples in unattended operation. To achieve these conditions, reliability and reproducibility are a prerequisite. Our current protocol incorporates a TiO₂ recovery step, in which, after TiO₂ elution with a high pH solution, 20 μ L of 5% formic acid is injected over the sandwich column. In this way, the TiO₂ precolumn is completely regenerated and allows multiple injections, showing no signs of reduced performance. Supple-

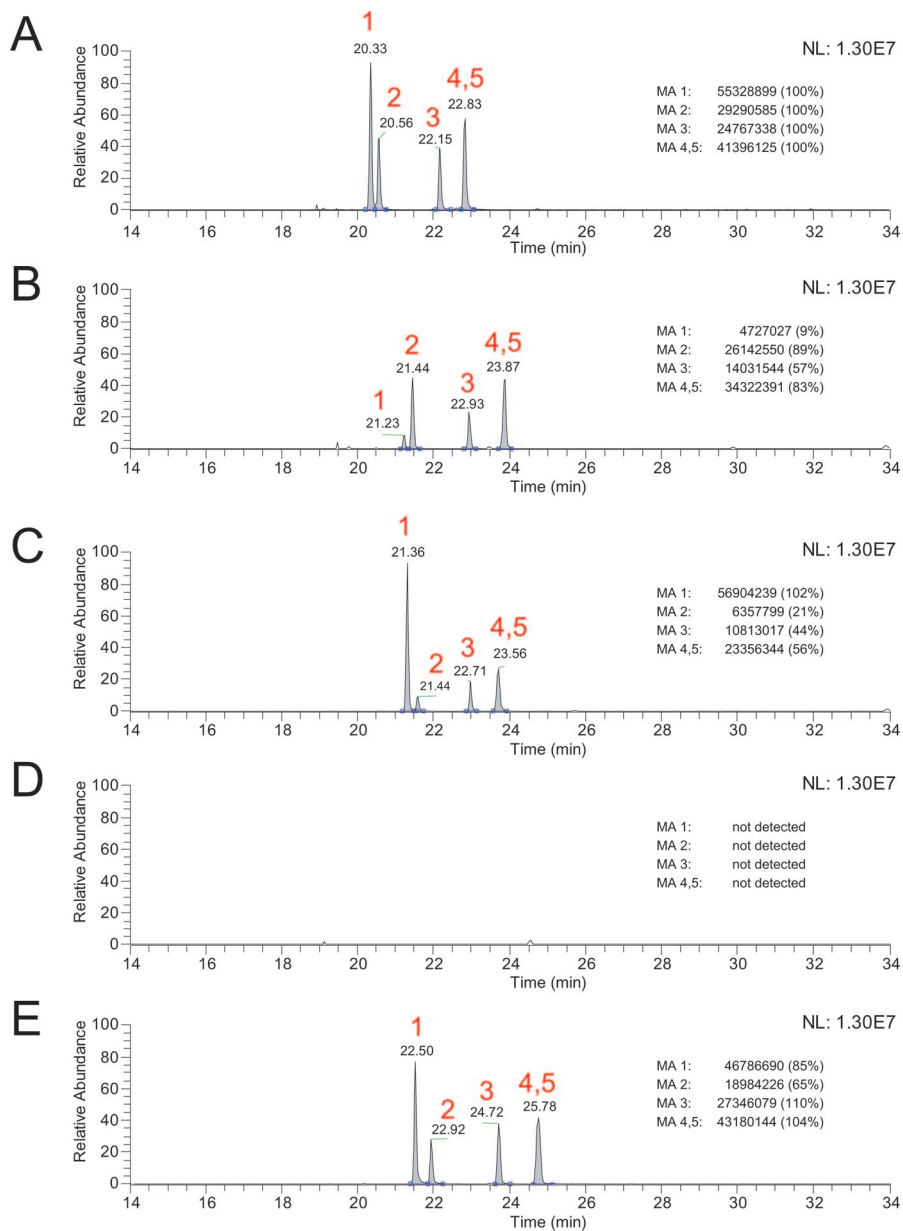


Figure 2. Extracted ion chromatograms of the 5 phosphorylated peptides from 25 fmol of the mixture of the digested (phospho)proteins beta- and alpha-caseins and the synthetic peptide. Chromatogram A shows the EIC for the analysis using standard RP-HPLC (i.e., using only a C18 precolumn to trap peptides) for comparison. Chromatograms B and C show the EICs for the analysis of the mixture using a double precolumn of 5 mm TiO₂ and 30 mm C18, wherein in B the flow-through fraction and in C the TiO₂ trapped fraction is given. The chromatograms D and E show the EICs for the analysis of the mixture using a triple precolumn of 30 mm C18, 5 mm TiO₂ and 30 mm C18, wherein in D the flow-through fraction and in E the TiO₂ trapped fraction is given. The intensities in the chromatograms are direct reflections of the peptide abundances. The extracted ion chromatograms were constructed by choosing the [M + 2H]²⁺ ions of FQpSEEQQTEDELQDK at *m/z* 1031.41 (1), the [M + 2H]²⁺ of RKlpSASEF at *m/z* 509.24 (2), the [M + 2H]²⁺ of TVDMEpSTEVFTK at *m/z* 733.81 (3), the [M + 2H]²⁺ of VPQLEIVPNpSAEER at *m/z* 830.90 (4), the [M + 3H]³⁺ of YKVPQLEIVPNpSAEER at *m/z* 651.32 (5). Absolute values for peak areas as listed in each chromatogram. The relative recovery in each chromatogram was calculated by setting the C18-only chromatogram (A) at 100%.

mentary Figure 2 in Supporting Information shows 6 repetitive runs of 25 fmol of the standard mixture. No breakthrough of any of the phosphopeptides from the test mixture was observed, even after multiple analyses (data not shown). The extracted ion chromatograms of the TiO₂ eluate demonstrate the reproducibility of 2D-LC setup. To test the applicability of the method in large-scale analyses of phosphorylated peptides from total cellular extracts, we prepared and analyzed a total cellular extract of cultured *D. melanogaster* S2 cells using a MudPit strategy. Proteolytic peptides were first subjected to

SCX chromatography. This chromatographic separation has been previously shown to substantially enrich for phosphorylated tryptic peptides due to their overall lower net solution-charge at low pH.¹⁸ Each SCX fraction (24 in total) was split into four and analyzed by LC-MS analysis only or by the online phosphopeptide enrichment approach. From the 24 SCX fractions, a total of 549 phosphorylated peptides were detected by RP-LC-MS only. When the TiO₂ approach was used, a total of 2152 unique phosphorylated peptides were identified. In total, only 55 phosphopeptides were identified in the flow-

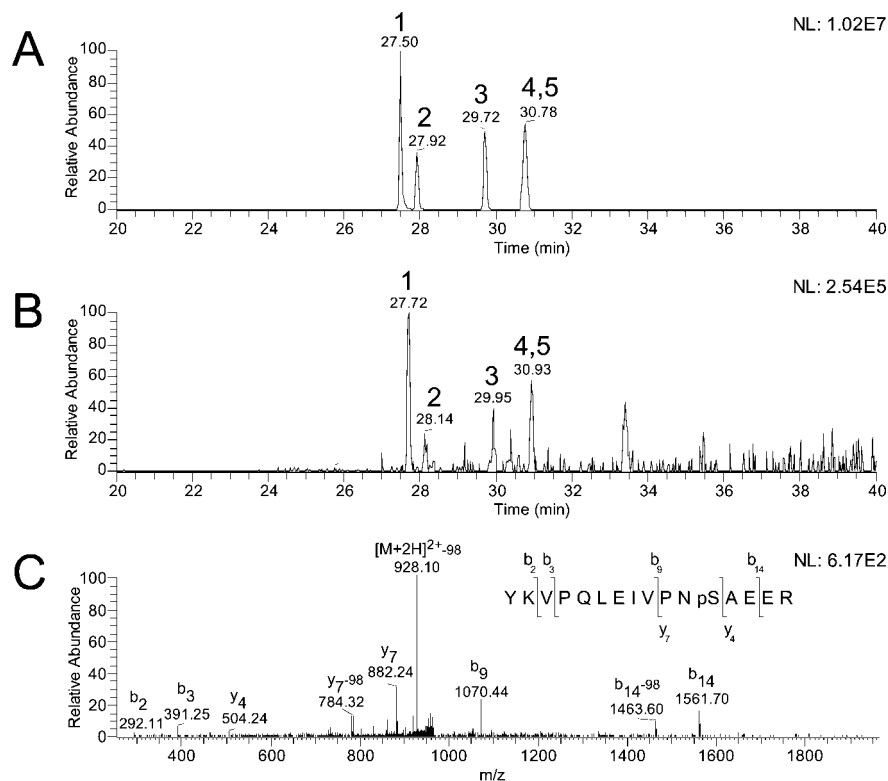


Figure 3. Extracted ion chromatogram of the 5 phosphorylated peptides of an analysis of (A) 25 fmol and (B) 500 amol of the (phospho)protein and peptide mixture. This latter analysis was still sufficient to obtain good quality MS² spectra for unambiguous identification of all 5 phosphopeptides, as illustrated for the alpha-casein peptide YKVPQLEIVPNpSAEER in panel C. Phosphopeptide-labelling is identical as in Figure 2.

through analyses of all 24 SCX fractions. Thirty-one of these flow-through peptides were also among the 2152 identified in the TiO₂ elution. These results are summarized in Venn diagrams depicted in Figure 4A. The above results show that online TiO₂ enrichment of SCX-fractionated peptides results in a 4-fold increase of detected phosphorylated peptides, when compared to SCX alone. In certain SCX-fractions, we detected a superior enrichment level. For example, when subjected to RP-LC–MS directly, SCX-fraction 7 yielded only 84 identified phosphorylated peptides, while the base peak chromatogram (Figure 4B, top chromatogram) suggests that this particular fraction contains a large amount of peptides. This particular SCX fraction represents the singly charged peptides in SCX, and contains primarily C-terminally and N-terminally acetylated peptides, but is also expected to contain phosphorylated peptides. When the same fraction was subjected to the online-TiO₂ setup, 624 phosphorylated peptides were identified in the TiO₂-eluate, whereas only 31 nonphosphorylated peptides were identified within this 70 min LC–MS analysis. Additionally, no phosphorylated peptides were detected in the flow-through, whereas the base peak intensity chromatogram (Figure 4B, middle chromatogram) of the flow-through is equally intense as a normal RP-LC–MS analysis. The base peak chromatogram of the TiO₂-eluate (Figure 4B, bottom chromatogram) is substantially lower than the flow-through and, as mentioned above, contains almost exclusively phosphorylated peptides, highlighting the superior enrichment for this particular fraction. This superior enrichment level is not reached for all fractions; for certain others, nonphosphorylated peptides are detected within the TiO₂ eluate, particularly highly abundant peptides.

In other words, the usage of formic acid reduces the nonspecific binding of acidic phosphopeptides, but it does not completely abolish it.

Comparison with Off-Line TiO₂ Enrichment Using DHB.

It has been shown several times that highly selective enrichment of phosphorylated peptides can be achieved when using DHB during the sample loading.^{11,13,21} This procedure yields reasonably ‘pure’ phosphopeptide fractions, but due to the high concentration of DHB in the final sample, they are less suitable for direct analysis by LC-ESI–MS, as the DHB is known to contaminate the LC and/or ion source of the mass spectrometer.^{13,15} To compare the performance of our online setup with the off-line DHB-TiO₂ approach, we analyzed four of the most complex SCX fractions (numbers 10–13) via the off-line DHB-TiO₂ approach. These fractions are of extremely high complexity; that is, they represent the 2+–SCX fractions, containing a large amount of ‘standard’ tryptic peptides, making the enrichment of the phosphopeptides difficult and essential. Still, in both the online TiO₂ and the off-line TiO₂/DHB approaches we found similar numbers of phosphorylated peptides, 464 using the online method and 508 via the offline DHB method (see Supplementary Figure 3 in Supporting Information). However, the number of nonphosphorylated peptides was substantially lower with the off-line DHB approach. More surprisingly, we observed that the overlap of detected phosphorylated peptides was no more than 30% (see Supplementary Figure 3 in Supporting Information) for each fraction, indicating that both phosphopeptide enrichment methods are still far from being comprehensive. As mentioned, the fractions analyzed contain the 2+–SCX fraction of tryptic peptides, which are by far the largest fraction of peptides within this particular

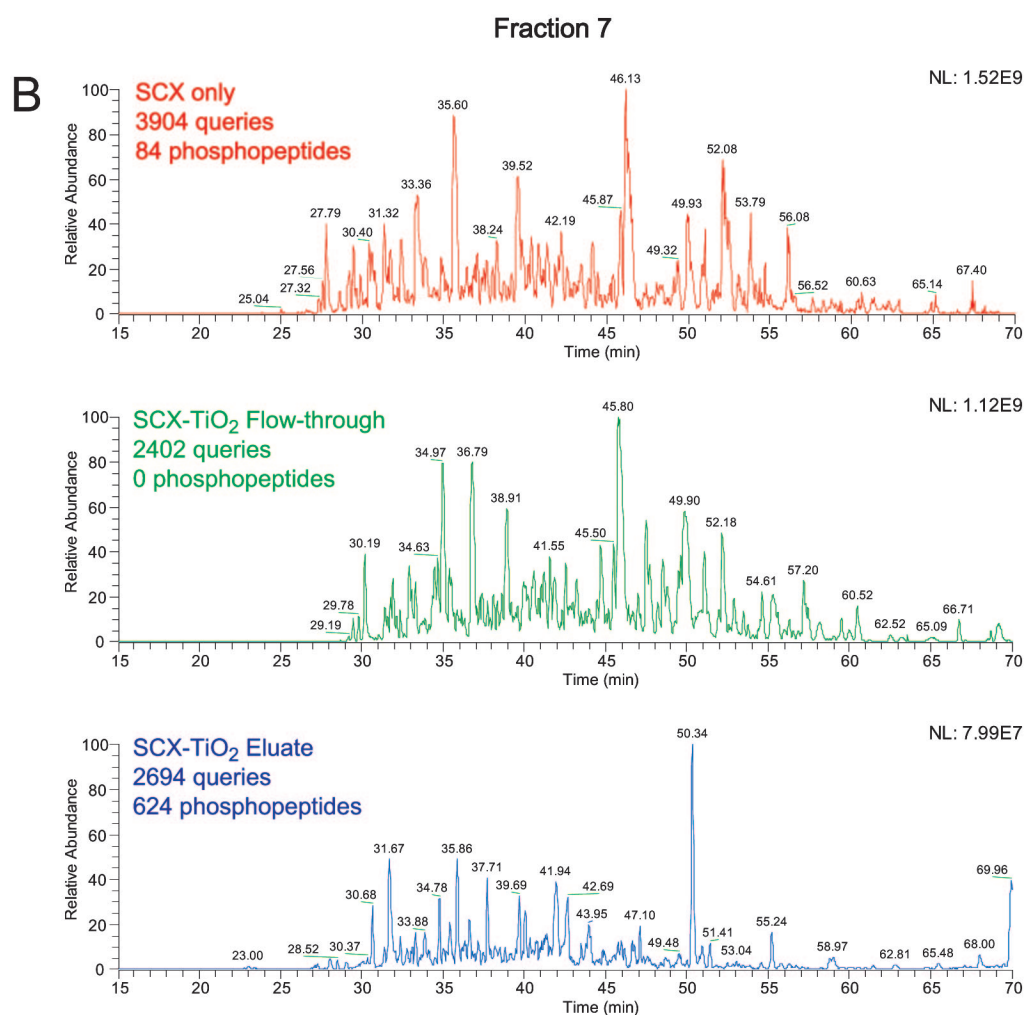
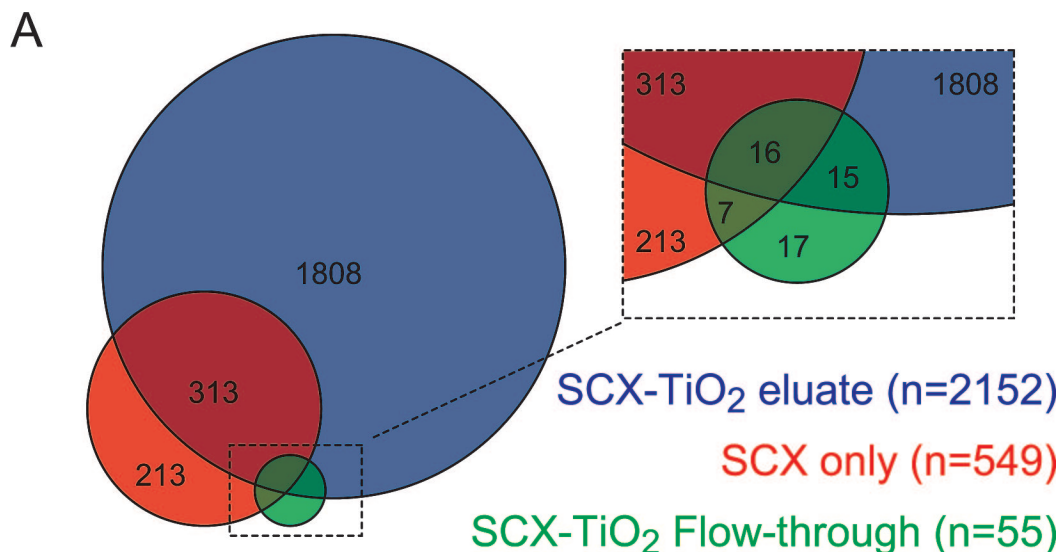


Figure 4. (A) Schematic overview of the overlap between identified phosphopeptides from (red) SCX-LC-MS, from the flow-through (green), and eluate (blue) of the SCX-online TiO₂ approach. (B) Base peak intensity chromatograms of the analysis of SCX fraction 7. Shown are the reversed phase analysis only (top) and the flow-through (middle) and the eluate (bottom) of the online TiO₂ approach. The number for queries and the number of identified phosphopeptides are given.

sample. Hence, a substantial contribution to this poor overlap results from oversampling of the mass spectrometer. For such complex samples, it is advisory to either perform further

fractionation or to analyze the same sample multiple times. In addition, the off-line method has evidently a larger dynamic range as compared to the online method. This is largely due

to the problem of overloading the reversed-phase column system and subsequent carryover and detection of abundant peptides for the flow-through to the TiO₂-elution. If this latter is the case, an additional H₂O/MeCN gradient prior to TiO₂-elution can be performed to obtain a better separation. Although this example is an extreme case and better enrichment/recovery is usually obtained for either two techniques on less complex samples, it shall be clear that both the online TiO₂ enrichment and the off-line TiO₂ approach with DHB are far from comprehensive, as illustrated by the poor overlap. In the Discussion, we will describe several factors that may cause bias in phosphoproteomics analysis and evaluate which of these still leave room for further improvement.

Discussion

Reversible protein phosphorylation ranks among the most important post-translational modifications that occur in the cell. Therefore, the characterization of phosphorylation events is a highly relevant, albeit a highly challenging, task. Significant progress surrounding the biochemical analysis of reversible protein phosphorylation in the past five years has led to the development of several new techniques to isolate and/or enrich phosphopeptides, enabling large-scale analyses. It is however evident that even with these major advances the analysis of a cellular phosphoproteome by current technologies is still far from being comprehensive. Many experimental factors influence the efficiency and reproducibility of current phosphopeptide enrichment strategies, such as sample loading speed, loading, and elution solvents; completeness of digestion; the nature of the solid phase material; and so forth. In a manual approach, all these factors are more difficult to control, leading to issues in reproducibility and robustness. Moreover, current enrichment techniques are still not sufficiently specific, often also biased toward the enrichment of specific classes of phosphopeptides, such as singly phosphorylated peptides or phosphopeptides that are either more acidic or basic. Here, we seek to evaluate some of these parameters in more detail in order to develop a more robust method that is relatively unbiased, albeit very sensitive and amendable to automation. We will first discuss the improvements introduced in Results in the context of previously reported modifications to the enrichment technique, and then highlight some of the parameters that lead to nonspecificity and bias in phosphopeptide enrichment techniques, primarily focusing on the isoelectric points profiles of the enriched phosphopeptides.

Schlosser et al.³¹ previously showed that a relatively high level of formic acid (2–5%) enhances the selectivity of enrichment of phosphorylated peptides on TiO₂ and substantially reduced the binding of nonphosphorylated peptides with an acidic character. In agreement with Schlosser et al.,³¹ we observed a reduction in nonspecific binding with the addition of 0.5% formic acid in our online approach, although at the expense of a diminished recovery of phosphorylated peptides. Instead, a large fraction of phosphorylated peptides were detected among the majority of nonphosphorylated peptides in the ‘breakthrough’ fractions. It became quite obvious that the actual sample loading flow-rate, which was 3 μL min⁻¹, formed a critical determinant in binding efficiency of the phosphorylated peptides. This was also noted by Schlosser et al., who used a loading flow rate of 1 μL min⁻¹. Although reducing the sample loading flow rate enhances the adsorption of phosphorylated peptides, a major drawback is the increase in total analysis time for each sample, especially those with

large sample volumes. To maintain a high throughput and enhance adsorption of phosphorylated peptides, we envisioned that an additional C18 trapping column would enable us to benefit from both issues. An additional advantage is that samples may then be first desalted prior to loading onto the TiO₂-precolumn, which effectively removes compounds potentially present in the sample that could interfere in the phosphopeptide-TiO₂ loading step. The high capacity of TiO₂ in combination with the ‘sandwich’-precolumn combination, delivering optimal loading conditions, allows for much smaller TiO₂ bed volumes. The TiO₂ bed volume used is approximately 40 nL, which is much smaller than the bed volume of pipet tip based microcolumns, which are closer to 300 nL in volume. As a consequence, the basicity or ionic strength of the elution buffer in combination with the elution volume needed for high recovery from our small trap-columns are both lower and less stringent, when compared to off-line microcolumns. When the mixture of several hard Lewis bases and NH₄HCO₃ at a pH of 9.0 was used, very high recovery rates were achieved and minimal interference or contamination of LC-system or ion source was observed. Finally, the use of 0.5% formic acid in the solvent system, and an injection of 5% formic acid for regeneration, provided reproducible and robust analyses over long periods of time. Overall sensitivity of the system was demonstrated to reach the attomole level. The general applicability of the newly developed online-approach was tested by analyzing a total cellular tryptic digest of *D. melanogaster* S2 cells. Overall, in the online method, a total of 2176 phosphorylated peptides were identified, of which 2152 were retained and recovered from the sandwiched TiO₂ precolumn. Only 55 phosphopeptides were detected in the breakthrough, of which only 24 were exclusively detected in the breakthrough. In a direct comparison of the SCX-LC-MS and SCX-TiO₂-LC-MS approach, the TiO₂ enrichment led to a factor 4 higher number of detected phosphopeptides.

Several reports have hinted to the fact that the enrichment of phosphopeptides may be biased toward either more acidic or basic phosphopeptides.^{8,32–34} To investigate this more specifically, we calculated the *pI* profiles of all detected phosphopeptides. As described in Experimental Procedures, the *pI* values were calculated using an in-house built java tool, where the amino acid p*K*_a's were used as reported in refs 24 and 25, with the p*K*_a's for pY and pS/T taken from ref 26. We binned the calculated *pI*'s in three sets termed acidic, intermediate, and basic, with the limits set somewhat subjective from *pI* < 5 for the acidic, pH 5 < *pI* > pH 7 for the intermediate, and *pI* > 7 for the basic. Figure 5 shows several of these calculated *pI* profiles. In Figure 5A, we provide, for illustrative purposes, the *pI* profile of an *in silico* tryptic digest of the complete *D. melanogaster* protein database without phosphorylations or any other PTMs. This *pI* profile reveals multiple maxima and minima, whose existence have been confirmed by experimental data using large-scale peptide isoelectric focusing experiments.³⁵ In Figure 5B, the *pI* profile of the phosphorylated peptides bound and eluted using the sandwiched SCX-TiO₂-nanoLC-MS setup is given. We note that this profile resembles that of the total peptide lysates given in Figure 5A, evidently somewhat shifted toward acidic *pI*, caused by the presence of the negatively charged phosphate groups in these peptides. On average, the *pI* is lowered by 0.5 for a single phosphorylation event in acidic peptides and approximately 2–3 for the more basic peptides. We note that about 52% of all 1962 detected phosphopeptides are within the

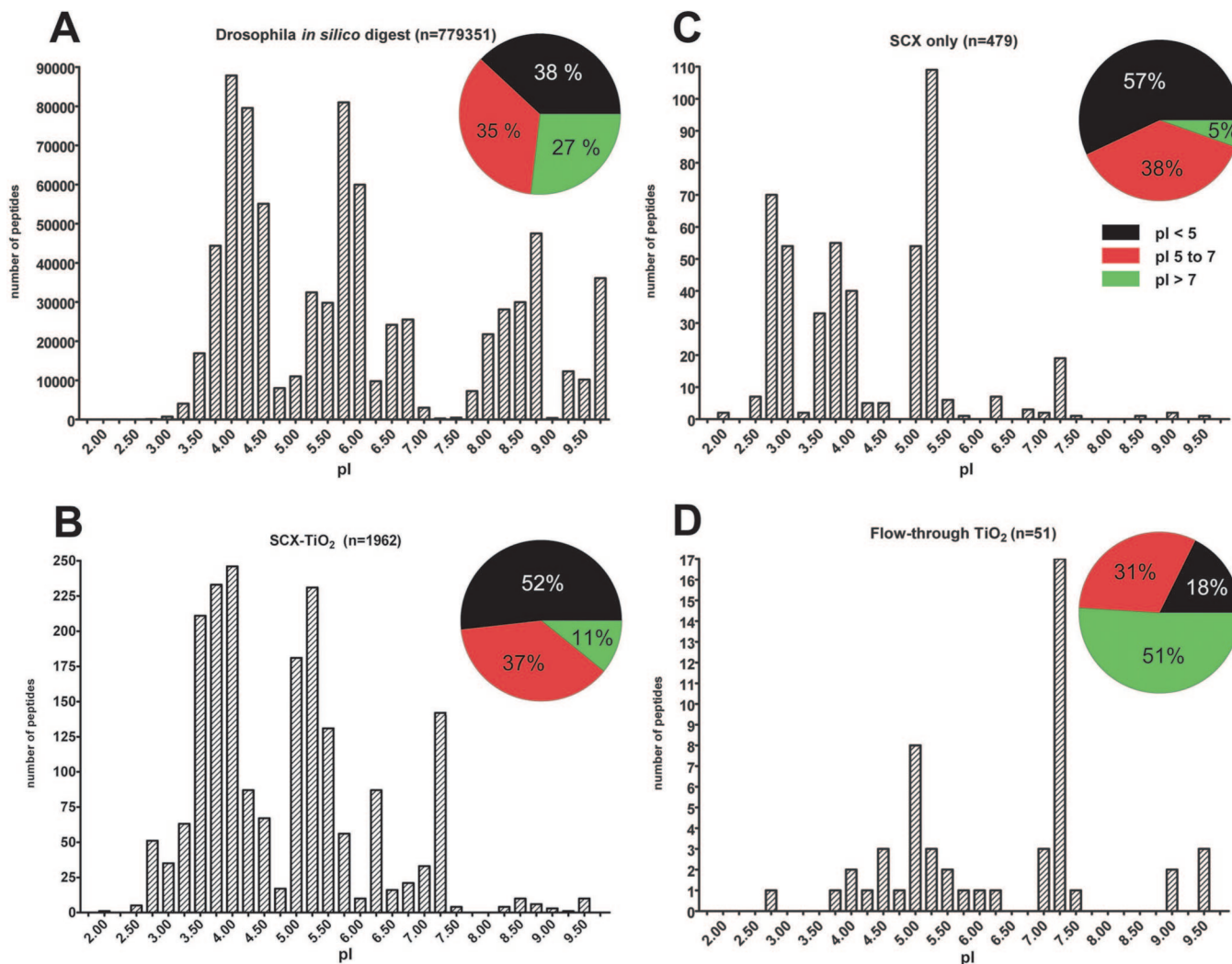


Figure 5. Peptide *pI* distributions for (A) an *in silico* tryptic digest of the *D. melanogaster* protein database without phosphorylations or any other PTMs, (B) phosphorylated peptides bound and eluted using SCX-TiO₂-nanoLC-MS, (C) phosphorylated peptides identified using SCX-LC-MS only, and (D) the phosphorylated peptides identified from the SCX-TiO₂-nanoLC specifically that did not bind to TiO₂ (i.e., the flow-through). The inset pie charts for each *pI* plot indicate the proportion of acidic, intermediate, and basic phosphopeptides, categorized using the limits *pI* < 5, *pI* 5–7, and *pI* > 7.

acidic category. For comparison, we depict in Figure 5C the *pI* profile of the 479 phosphorylated peptides identified using SCX-LC-MS only, which resembles that of Figure 5B to some extent, but is lacking some of the more basic phosphopeptides. Interestingly, the *pI* profile of the 51 phosphopeptides that did not bind to TiO₂ and were thus detected in the flow-through reveal a strong bias toward being “basic” phosphopeptides (Figure 5D), with 51% of the phosphopeptides being “basic”, indicating that with the current setup the TiO₂ lacks trapping efficiency for these classes of phosphopeptides. This agrees well with a systematic analysis done by Klemm et al.,³² which reported on reduced binding efficiency of TiO₂ for phosphopeptides carrying multiple basic residues. For comparison, we calculated the *pI* profiles of recently reported large-scale phosphoproteomics experiments, which are given in the Supplementary Figure 4 in Supporting Information. We calculated and compared with our data set (Supplementary Figure 4A in Supporting Information) the *pI* profiles of the phosphorylated peptides identified in a mouse liver phosphoproteome study using extended shallow SCX gradients and IMAC performed by Villén et al.²⁸ (Supplementary Figure 4B in Supporting

Information), the phosphorylated peptides identified (taking a Mascot threshold score > 35) in a cell signaling study using SCX fractionation and off-line TiO₂ with DHB performed by Olsen et al.²⁹ (Supplementary Figure 4C in Supporting Information), and the phosphorylated peptides identified by Bodenmiller et al. when they evaluated multiple phosphopeptide enrichment techniques. Specifically, we highlight in Supplementary Figure 4D (Supporting Information) the profile of the peptides that were specifically enriched using IMAC in a batch mode.²⁷ The obtained *pI* profiles are strikingly different, revealing the bias of all these methods. Strikingly, whereas the ratio between basic and acidic phosphopeptides is 11:52% in our data set, it is 1:82% in the data set of Villén et al. It is fair to mention that due to the nature of their approach, the data set of Villén et al. is expected to be biased, since they primarily focus on phosphopeptides from the 1+ SCX fractions, as previously described.¹⁸ IMAC is not by itself the cause of the serious bias, and this becomes clear when considering the *pI* profile of Bodenmiller et al. that revealed a ratio between acidic and basic phosphopeptides of 12:57%. In the large-scale analysis of Olsen et al. using SCX fractionation and off-line TiO₂

with DHB, the ratio between acidic and basic phosphopeptides was found to be 5:78%, again revealing a bias toward the detection of acidic peptides. Finally, we also evaluated the *pI* profiles of the data sets obtained in our own experiments on the selected SCX fractions whereby we aimed to compare the online TiO₂ and off-line TiO₂ DHB methods. Although, as mentioned above, these two limited data sets showed only 30% overlap, their corresponding *pI* profiles are fairly similar (Supplementary Figure 3 in Supporting Information). The fact that the overlap is very poor illustrates very clearly the 'imperfectness' of all phosphopeptide enrichment strategies. Obviously, currently no single enrichment technique is superior over the other, although the *pI* profiles observed using 'our' method pleasingly resembles the profile of an *in silico* tryptic digest of the complete *D. melanogaster* protein database. It does however reveal that all current phosphopeptide enrichment techniques are still far from being comprehensive and do not allow for complete analysis of the phosphoproteome, as is sometimes suggested. For comprehensive phosphoproteomic analysis, the prefractionation step is very important, and possibly more than one strategy should be used.³⁴ It should also be mentioned that the use of multiple proteolytic agents yields far higher sequence coverage, and subsequently will provide more of phosphorylation site identifications.^{2,31,36} Most current phosphopeptides enrichment strategies are frequently solely used in combination with trypsin. Trypsin alone will certainly generate phosphopeptides that are either too large or simply too small for successful chromatographic focusing and mass spectrometric detection. In particular, since many protein kinase motifs contain basic residues, such as arginine and lysine, subsequently, proteolytic cleavage with trypsin yields too small, or if the presence of the phospho moiety will render tryptic cleavage, too large and more basic phosphopeptides. Here, we present a method that is (relatively) not biased against either acidic or basic residues and is expected to be complementary with other proteolytic agents. The use of multiple proteolytic reagents, in combination with a robust phosphopeptide method, with high sensitivity and without bias against a particular type of peptides, will ultimately result in high recovery levels of the full phosphoproteome.

Conclusions

An optimized and automated online TiO₂-based liquid chromatographic approach, aimed at enriching phosphorylated peptides from large complex proteolytic digests, is described. With the use of a 'sandwich' C18-TiO₂-C18 precolumn, highly efficient phosphopeptide-loading conditions are achieved. A major advantage of this new setup is the very low flow by which phosphorylated peptides are loaded onto the TiO₂-precolumn, which results in very low levels of breakthrough, and more importantly is without any compromise on sample loading or analysis times. Another advantage inherent to the online approach is that it allows the complementary measurement of phosphopeptides and their nonphosphorylated counterparts in subsequent analyses, making the method well-suited for quantitative phosphoproteomics. The automated procedure was tested for sensitivity and reproducibility, and the obtained results demonstrate its potential for automated high-throughput analysis in large-scale phosphoproteomic analysis. Improved trapping and elution conditions were met by employing a triple stage precolumn, with a very small TiO₂ bed volume, and by using a combination of hard Lewis bases in combination with high pH in the elution step. The general applicability was

demonstrated using a cellular extract of *D. melanogaster* S2. This latter analysis demonstrates the selectivity of the method over a broad range of phosphorylated peptides, differing both in size, number of modified residues, and the primary amino acid sequence.

Abbreviations: 2D-LC, two-dimensional liquid chromatography; DHB, 2,5-dihydroxybenzoic acid; DTT, dithiothreitol; EIC, extracted ion chromatogram; IMAC, immobilized metal-ion affinity chromatography; MS, mass spectrometry; *pI*, isoelectric point; SCX, strong cation exchange; TiO₂, titanium dioxide.

Acknowledgment. This work was supported by The Netherlands Proteomics Centre www.netherlandsproteomics-centre.nl.

Supporting Information Available: Extracted ion chromatograms of TiO₂-flowthrough and of TiO₂-eluate, to highlight the effect of different elution conditions, extracted ion chromatograms of TiO₂-eluates of multiple analysis, illustrating the reproducibility of the presented method, Venn diagrams showing the direct comparison of the online TiO₂ approach versus the off-line TiO₂-DHB approach, a figure showing the comparison of *pI* distributions of several large-scale phosphoproteomics studies, the paper recording of the UV-chromatogram of the strong cation exchange separation and a bar chart to illustrate the distribution of phosphopeptides over the SCX-separation. This material is available free of charge via the Internet at <http://pubs.acs.org>. All MS/MS spectra of the *D. melanogaster* experiment are available at https://bioinformatics.chem.uu.nl/supplementary/pinkse_JPR/ in one single scaffold file with an appropriate reader. This file contains all the information on peptide sequences and information on the PTMs.

References

- (1) Morandell, S.; Stasyk, T.; Grosstessner-Hain, K.; Roitinger, E.; Mechtler, K.; Bonn, G. K.; Huber, L. A. Phosphoproteomics strategies for the functional analysis of signal transduction. *Proteomics* **2006**, *6* (14), 4047–4056.
- (2) Pinkse, M. W. H.; Heck, A. J. R. Essential enrichment strategies in phosphoproteomics. *Drug Discovery Today: Technol.* **2006**, *3* (3), 331–337.
- (3) Reinders, J.; Sickmann, A. State-of-the-art in phosphoproteomics. *Proteomics* **2005**, *5* (16), 4052–4061.
- (4) Garcia, B. A.; Shabanowitz, J.; Hunt, D. F. Analysis of protein phosphorylation by mass spectrometry. *Methods* **2005**, *35* (3), 256–264.
- (5) Jensen, O. N. Interpreting the protein language using proteomics. *Nat. Rev. Mol. Cell Biol.* **2006**, *7* (6), 391–403.
- (6) Mann, M.; Jensen, O. N. Proteomic analysis of post-translational modifications. *Nat. Biotechnol.* **2003**, *21* (3), 255–261.
- (7) Posewitz, M. C.; Tempst, P. Immobilized gallium(III) affinity chromatography of phosphopeptides. *Anal. Chem.* **1999**, *71* (14), 2883–2892.
- (8) Ficarro, S. B.; McClelland, M. L.; Stukenberg, P. T.; Burke, D. J.; Ross, M. M.; Shabanowitz, J.; Hunt, D. F.; White, F. M. Phosphoproteome analysis by mass spectrometry and its application to *Saccharomyces cerevisiae*. *Nat. Biotechnol.* **2002**, *20* (3), 301–305.
- (9) Pinkse, M. W.; Uitto, P. M.; Hilhorst, M. J.; Ooms, B.; Heck, A. J. Selective isolation at the femtomole level of phosphopeptides from proteolytic digests using 2D-NanoLC-ESI-MS/MS and titanium oxide precolumns. *Anal. Chem.* **2004**, *76* (14), 3935–3943.
- (10) Kuroda, I.; Shintani, Y.; Motokawa, M.; Abe, S.; Furuno, M. Phosphopeptide-selective column-switching RP-HPLC with a titanium precolumn. *Anal. Sci.* **2004**, *20* (9), 1313–1319.
- (11) Larsen, M. R.; Thingholm, T. E.; Jensen, O. N.; Roepstorff, P.; Jorgensen, T. J. Highly selective enrichment of phosphorylated peptides from peptide mixtures using titanium dioxide microcolumns. *Mol. Cell. Proteomics* **2005**, *4* (7), 873–886.
- (12) Stensballe, A.; Andersen, S.; Jensen, O. N. Characterization of phosphoproteins from electrophoretic gels by nanoscale Fe(III)

- affinity chromatography with off-line mass spectrometry analysis. *Proteomics* **2001**, *1* (2), 207–222.
- (13) Thingholm, T. E.; Jorgensen, T. J. D.; Jensen, O. N.; Larsen, M. R. Highly selective enrichment of phosphorylated peptides using titanium dioxide. *Nat. Protocols* **2006**, *1* (4), 1929–1935.
- (14) Kweon, H. K.; Hakansson, K. Selective zirconium dioxide-based enrichment of phosphorylated peptides for mass spectrometric analysis. *Anal. Chem.* **2006**, *78* (6), 1743–1749.
- (15) Mazanek, M.; Mitulovi, A. G.; Herzog, F.; Stingl, C.; Hutchins, J. R. A.; Peters, J.-M.; Mechtler, K. Titanium dioxide as a chemo-affinity solid phase in offline phosphopeptide chromatography prior to HPLC-MS/MS analysis. *Nat. Protocols* **2006**, *1* (4), 1977–1987.
- (16) Ficarro, S. B.; Salomon, A. R.; Brill, L. M.; Mason, D. E.; Stettler-Gill, M.; Brock, A.; Peters, E. C. Automated immobilized metal affinity chromatography/nano-liquid chromatography/electrospray ionization mass spectrometry platform for profiling protein phosphorylation sites. *Rapid Commun. Mass Spectrom.* **2005**, *19* (1), 57–71.
- (17) Wang, J.; Zhang, Y.; Jiang, H.; Cai, Y.; Qian, X. Phosphopeptide detection using automated online IMAC-capillary LC-ESI-MS/MS. *Proteomics* **2006**, *6* (2), 404–411.
- (18) Beausoleil, S. A.; Jedrychowski, M.; Schwartz, D.; Elias, J. E.; Villen, J.; Li, J.; Cohn, M. A.; Cantley, L. C.; Gygi, S. P. Large-scale characterization of HeLa cell nuclear phosphoproteins. *Proc. Natl. Acad. Sci. U.S.A.* **2004**, *101* (33), 12130–12135.
- (19) Gruhler, A.; Olsen, J. V.; Mohammed, S.; Mortensen, P.; Faergeman, N. J.; Mann, M.; Jensen, O. N. Quantitative phosphoproteomics applied to the yeast pheromone signaling pathway. *Mol. Cell. Proteomics* **2005**, *4* (3), 310–327.
- (20) Trinidad, J. C.; Specht, C. G.; Thalhammer, A.; Schoepfer, R.; Burlingame, A. L. Comprehensive identification of phosphorylation sites in postsynaptic density preparations. *Mol. Cell. Proteomics* **2006**, *5* (5), 914–922.
- (21) Benschop, J. J.; Mohammed, S.; O’Flaherty, M.; Heck, A. J.; Slijper, M.; Menke, F. L. Quantitative phospho-proteomics of early elicitor signalling in *Arabidopsis*. *Mol. Cell. Proteomics* **2007**, *6*, 1198–1214.
- (22) Rappsilber, J.; Ishihama, Y.; Mann, M. Stop and go extraction tips for matrix-assisted laser desorption/ionization, nanoelectrospray, and LC/MS sample pretreatment in proteomics. *Anal. Chem.* **2003**, *75* (3), 663–670.
- (23) Elias, J. E.; Haas, W.; Faherty, B. K.; Gygi, S. P. Comparative evaluation of mass spectrometry platforms used in large-scale proteomics investigations. *Nat. Methods* **2005**, *2* (9), 667–75.
- (24) Bjellqvist, B.; Basse, B.; Olsen, E.; Celis, J. E. Reference points for comparisons of two-dimensional maps of proteins from different human cell types defined in a pH scale where isoelectric points correlate with polypeptide compositions. *Electrophoresis* **1994**, *15* (3–4), 529–539.
- (25) Bjellqvist, B.; Hughes, G. J.; Pasquali, C.; Paquet, N.; Ravier, F.; Sanchez, J. C.; Frutiger, S.; Hochstrasser, D. The focusing positions of polypeptides in immobilized pH gradients can be predicted from their amino acid sequences. *Electrophoresis* **1993**, *14* (10), 1023–1031.
- (26) Kumar, Y.; Khachane, A.; Belwal, M.; Das, S.; Somsundaram, K.; Tatu, U. ProteoMod: A new tool to quantitate protein post-translational modifications. *Proteomics* **2004**, *4* (6), 1672–1683.
- (27) Bodenmiller, B.; Mueller, L. N.; Mueller, M.; Domon, B.; Aebersold, R. Reproducible isolation of distinct, overlapping segments of the phosphoproteome. *Nat. Methods* **2007**, *4* (3), 231–237.
- (28) Villen, J.; Beausoleil, S. A.; Gerber, S. A.; Gygi, S. P. Large-scale phosphorylation analysis of mouse liver. *Proc. Natl. Acad. Sci. U.S.A.* **2007**, *104* (5), 1488–1493.
- (29) Olsen, J. V.; Blagoev, B.; Gnäd, F.; Macek, B.; Kumar, C.; Mortensen, P.; Mann, M. Global, in vivo, and site-specific phosphorylation dynamics in signaling networks. *Cell* **2006**, *127* (3), 635–648.
- (30) Sugiyama, N.; Masuda, T.; Shinoda, K.; Nakamura, A.; Tomita, M.; Ishihama, Y. Phosphopeptide enrichment by aliphatic hydroxy acid-modified metal oxide chromatography for NanoLC-MS/MS in proteomics applications. *Mol. Cell. Proteomics* **2007**, *6*, 1103–1109.
- (31) Schlosser, A.; Vanselow, J. T.; Kramer, A. Mapping of phosphorylation sites by a multi-protease approach with specific phosphopeptide enrichment and NanoLC-MS/MS analysis. *Anal. Chem.* **2005**, *77* (16), 5243–5250.
- (32) Klemm, C.; Otto, S.; Wolf, C.; Haseloff, R. F.; Beyermann, M.; Krause, E. Evaluation of the titanium dioxide approach for MS analysis of phosphopeptides. *J. Mass Spectrom.* **2006**, *41* (12), 1623–1632.
- (33) Nuhse, T. S.; Stensballe, A.; Jensen, O. N.; Peck, S. C. Large-scale analysis of in vivo phosphorylated membrane proteins by immobilized metal ion affinity chromatography and mass spectrometry. *Mol. Cell. Proteomics* **2003**, *2* (11), 1234–1243.
- (34) Dai, J.; Jin, W. H.; Sheng, Q. H.; Shieh, C. H.; Wu, J. R.; Zeng, R. Protein phosphorylation and expression profiling by Yin-yang multidimensional liquid chromatography (Yin-yang MDLC) mass spectrometry. *J. Proteome Res.* **2007**, *6* (1), 250–262.
- (35) Krijgsveld, J.; Gauci, S.; Dormeyer, W.; Heck, A. J. In-gel isoelectric focusing of peptides as a tool for improved protein identification. *J. Proteome Res.* **2006**, *5* (7), 1721–1730.
- (36) Jones, D. R.; Bultsma, Y.; Keune, W. J.; Halstead, J. R.; Elouarrat, D.; Mohammed, S.; Heck, A. J.; D’Santos, C. S.; Divecha, N. Nuclear PtdIns5P as a transducer of stress signaling: an in vivo role for PIP4Kbeta. *Mol. Cell* **2006**, *23* (5), 685–695.

PR700605Z